Journal of Alloys and Compounds 509 (2011) 10150–10154

Contents lists available at SciVerse ScienceDirect

Journal of Alloys and Compounds

journal homepage: www.elsevier.com/locate/jallcom

Glycolthermal synthesis and characterization of hexagonal CdS round microparticles in flower-like clusters

Anukorn Phuruangrat[a,*], Nuengruethai Ekthammathat[b], Titipun Thongtem[b,d,**], Somchai Thongtem[c,d]

[a] Department of Materials Science and Technology, Faculty of Science, Prince of Songkla University, Hat Yai, Songkhla 90112, Thailand
[b] Department of Chemistry, Faculty of Science, Chiang Mai University, Chiang Mai 50200, Thailand
[c] Department of Physics and Materials Science, Faculty of Science, Chiang Mai University, Chiang Mai 50200, Thailand
[d] Materials Science Research Center, Faculty of Science, Chiang Mai University, Chiang Mai 50200, Thailand

ARTICLE INFO

Article history:
Received 11 August 2010
Received in revised form 14 August 2011
Accepted 16 August 2011
Available online 22 August 2011

Keywords:
Luminescence
Optical materials
Scanning electron microscopy
Transmission electron microscopy
X-ray diffraction

ABSTRACT

Hexagonal CdS round microparticles in flower-like clusters were synthesized by glycolthermal reactions of $CdCl_2$ and thiourea as cadmium and sulphur sources in 1,2-propylene glycol (PG) at 100–200 °C for 10–30 h. Phase and morphology were detected using X-ray diffraction (XRD), and scanning and transmission electron microscopy (SEM, TEM). The products were pure phase of hexagonal wurtzite CdS. The quantitative elemental analysis of Cd:S ratio was detected using energy dispersive X-ray (EDX) analyzer. Raman spectrometer revealed the presence of fundamental and overtone modes at 296 and 595 cm^{-1}, corresponding to the strong 1LO and weak 2LO modes, respectively. Photonic properties were investigated using UV–visible and photoluminescence (PL) spectroscopy. They showed the same absorption at 493–498 nm, and emission at 431 nm due to the excitonic recombination process. A possible formation mechanism was also proposed, according to experimental results.

1. Introduction

CdS is one of the most interesting II–VI compounds due to its potential use in solar cells, laser light-emitting diodes and photoelectronic devices [1]. Generally, materials with different morphologies have strong influence on their properties [2–4]. Among them are flower-like crystals [1,5,6], dendrites [7], nanorods [8], nanoparticles [3,4,9], microspheres [10], and hexagons and triangles [11]. Hence, controlling the shapes and sizes is still a major challenge. There have been different methods used for synthesizing the sulphide, such as hydrothermal and solvothermal processes [1,7,10,11], cyclic microwave radiation [5] and sonochemistry-assisted microwave synthesis [2]. Some additives may be used in the processes to function as surfactants, templates and others [3,9,10].

Previously, glycols have been used as solvents for the synthesis of well-dispersed particles by preventing the agglomeration process [12,13]. Those with dielectric constant (relative permittivity) of more than 30 are good in dissolving inorganic compounds [13]. Nucleation and growth of particles are able to proceed even at boiling points of the solvents [13]. Well-crystallized products, initiated by the high temperature process, have the influence on their properties. In general, polyols have low molecular masses and can be removed with ease. They functioned as weak stabilizers, which have the influences on the precipitation process. It is quite simple and can be used for large-scale synthesis. Comparing to water (heat capacity = 76 J mol^{-1} K^{-1}), 1,2-propylene glycol (PG) or 1,2-propanediol (boiling point = 187.6 °C, heat capacity = 190.8 J mol^{-1} K^{-1}) [14] is able to absorb more heat and retain the liquid phase at higher temperature. Therefore, PG was good choice for using as a solvent in the present process.

Hydrothermal is a synthetic process in a tightly closed system at high temperature and pressure, of which water is used as a solvent. When other organic solvents are used in the system, solvothermal is the preferential term. To specific focus on the use of 1,2-propylene glycol as a solvent, the term glycolthermal was thus used. The purpose of the present research is to glycolthermally synthesize hexagonal CdS round microparticles in flower-like clusters in PG without the use of any surfactants or additives. The effects of reaction temperatures and lengths of time under glycolthermal process on morphology and photoluminescence property of the products were also studied in more detail.

2. Experiment

To synthesize hexagonal CdS microparticles, each 0.005 mol of $CdCl_2$ and thiourea (NH_2CSNH_2) was dissolved in 16 ml 1,2-propylene

* Corresponding author. Tel.: +66 0 74 288374; fax: +66 0 74 288395.
** Corresponding author at: Department of Chemistry, Faculty of Science, Chiang Mai University, Chiang Mai 50200, Thailand. Tel.: +66 0 53 943344; fax: +66 0 53 892277.
E-mail addresses: phuruangrat@hotmail.com (A. Phuruangrat), ttpthongtem@yahoo.com (T. Thongtem).

0925-8388/$ – see front matter © 2011 Elsevier B.V. All rights reserved.
doi:10.1016/j.jallcom.2011.08.065

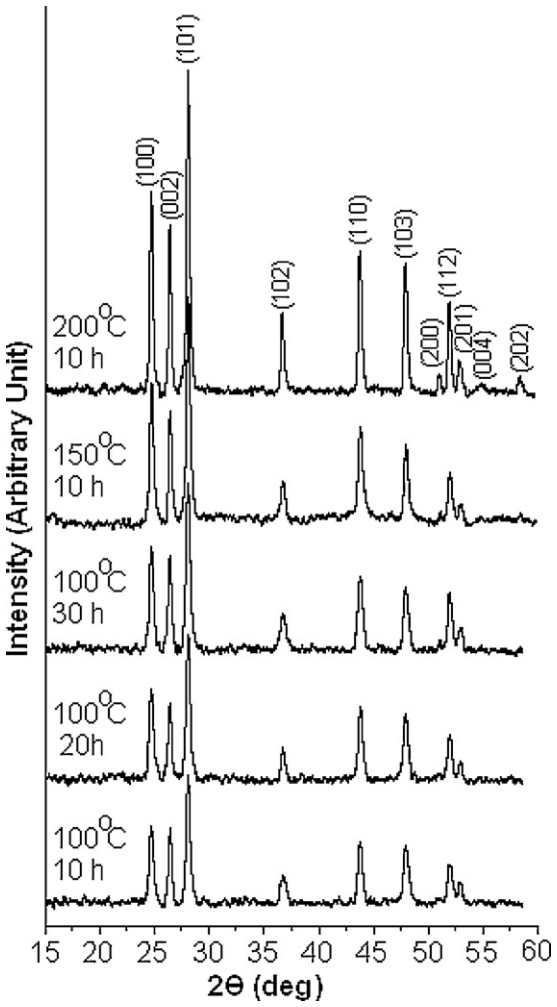

Fig. 1. XRD spectra of the products synthesized at different temperatures and times.

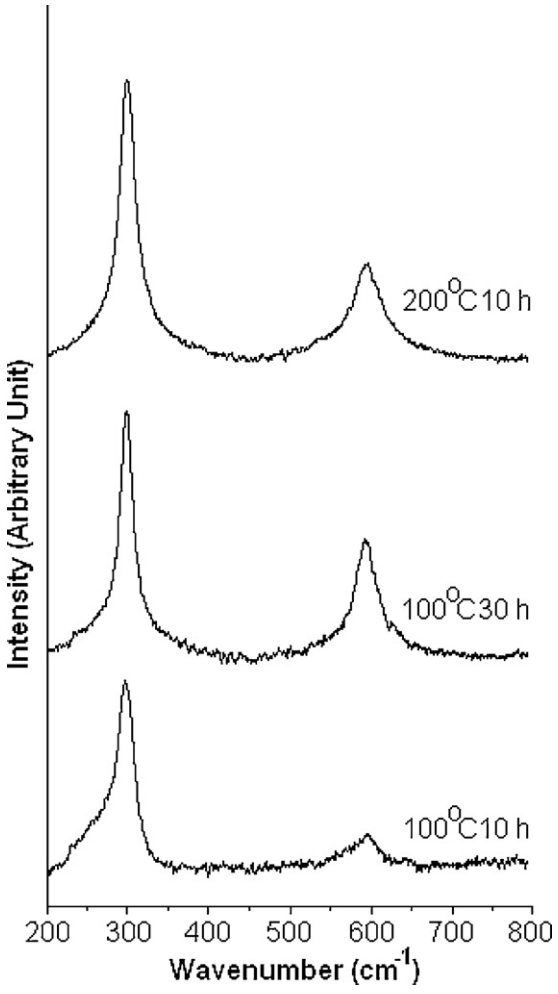

Fig. 2. Raman spectra of the products synthesized at different temperatures and times.

glycol (PG) or 1,2-propanediol ($C_3H_8O_2$) [14] under 30 min stirring at room temperature. Then the reactant solutions were filled in the lab-made Teflon-lined stainless steel autoclaves. They were tightly closed, heated by an electric oven at 100–200 °C for 10–30 h, and left cool down to room temperature. Finally, orange precipitates were synthesized, separated by filtration, washed with de-ionized water and absolute ethanol, and dried at 70 °C for 12 h.

The products were characterized using an X-ray diffractometer (XRD, SIEMENS D500) operating at 20 kV and 15 mA with K_α line from a copper target, a scanning electron microscope (SEM, JEOL JSM-6335F) equipped with an energy dispersive X-ray (EDX) analyzer operating at 15 kV, a transmission electron microscope (TEM, JEOL JEM-2010) and selected area electron diffractometer (SAED) operating at 200 kV, a Raman spectrometer (T64000 HORIBA Jobin Yvon) with 50 mW and 514.5 nm wavelength Ar green laser operating in the 200–800 cm^{-1} range, a UV–visible spectrometer (Lambda 25 PerkinElmer) with a UV lamp of 1 nm resolution, and a photoluminescence (PL) spectrometer (LS 50B PerkinElmer) with a 207 nm excitation wavelength (λ_{ex}) at room temperature.

3. Results and discussion

XRD spectra (Fig. 1) were indexed using Bragg's law for diffraction and compared with those of the JCPDS software (reference code: 06-0314) [15]. They were specified as hexagonal CdS ($a = b \neq c$, $\alpha = \beta = 90°$, $\gamma = 120°$) with $P6_3mc$ space group. The spectra are very sharp showing that well-crystallized particles were successfully synthesized [16,17]. No characteristic peaks of impurities were detected showing that each of the products was pure phase. XRD peaks were increased with the increase in the temperatures and prolonged times. Atoms aligned in systematic and symmetric order in the lattice, which resulted to higher XRD intensities. In the present research, the temperatures played more role in the intensities than the lengths of time did. Atoms were involved in violent vibration during the 100–200 °C and 10–30 h glycolthermal reactions. Their lattice parameters were calculated using the equation of plane spacing for hexagonal crystal and Bragg's law for diffraction [18]. They were $a = b = 0.4140$ nm, $c = 0.6738$ nm, very close to those of the JCPDS software [15].

A definite existence of hexagonal wurtzite CdS material was analyzed using a Raman spectrometer. The hexagonal wurtzite structured CdS belongs to the space group of C^4_{6V}. According to group theory calculation, the Raman active modes were $1A_1 + 1E_1 + 2E_2$ ($E_2{}^H$ and $E_2{}^L$), and the $2B_2$ modes were silent. For the A_1 branch, the phonon polarization was in the z direction. But for the doubly degenerate E_1 and E_2 branches, the phonon polarizations were in the xy plane. The wurtzite structure is noncentrosymmetric; therefore, both A_1 and E_1 modes split into longitudinal optical (LO) and transverse optical (TO) components [19]. Raman spectra of the as-synthesized CdS products are shown in Fig. 2. Two peaks were detected at the same wavenumbers of 296 and 595 cm^{-1} although the products were synthesized at different temperatures and lengths of time. These implied that the vibrations were independent of the synthesized conditions. They were controlled by the atomic masses of Cd and S, and their vibration constant. They are the first and second longitudinal optical (LO) phonon modes. The strong 1LO and weak 2LO were specified as the fundamental and overtone modes [19,20]. Coupling of the 1s–1s state to the LO phonon modes decreased with the decreasing of quantum crystallite size [20]. Some defects can play roles in the spectra as well.

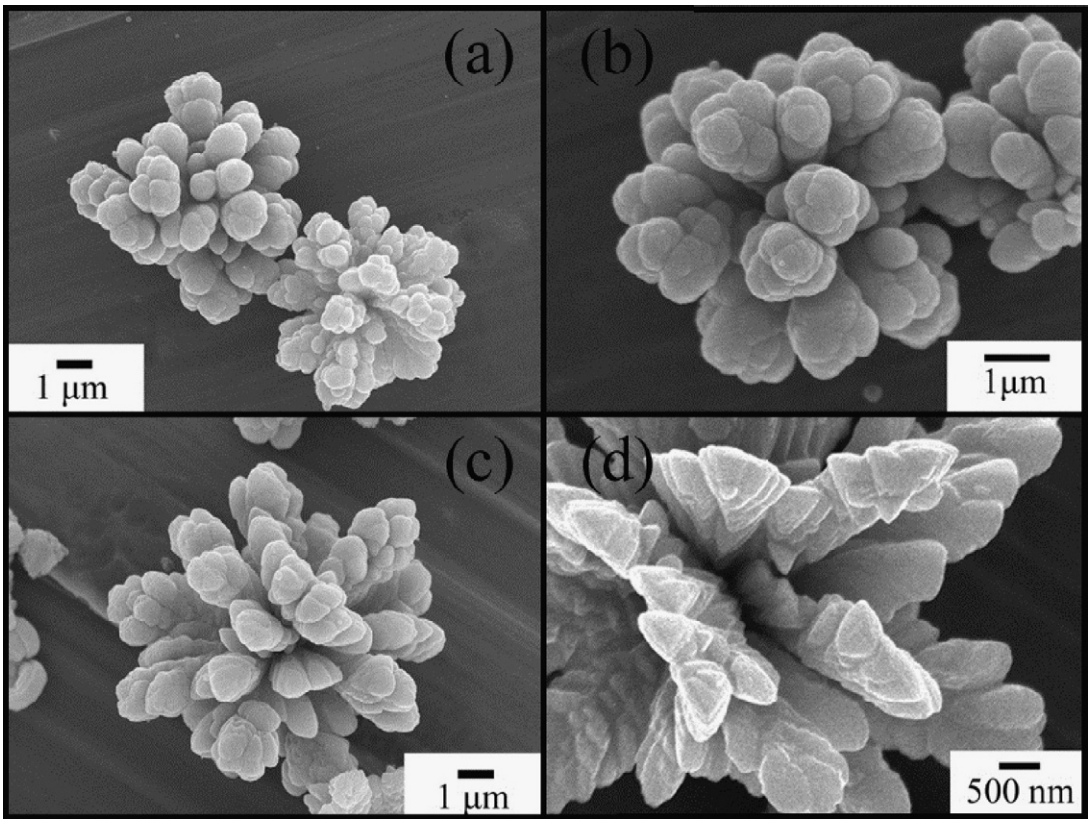

Fig. 3. SEM images at low and high magnifications of CdS synthesized at (a and b) 100 °C and (c and d) 200 °C for 10 h.

SEM images (Fig. 3) show that CdS products were composed of a number of round microparticles in flower-like clusters. Hexagonal CdS unit cells were aggregated into a number of nanoparticles composing round microparticles of which the sizes were limited by vapor pressure inside the autoclaves. The prolonged times (results not shown) did not play the significant role in the sizes of clusters as the temperatures did. The clusters became larger at higher temperature. At 200 °C for 10 h, the cluster was 10 μm in

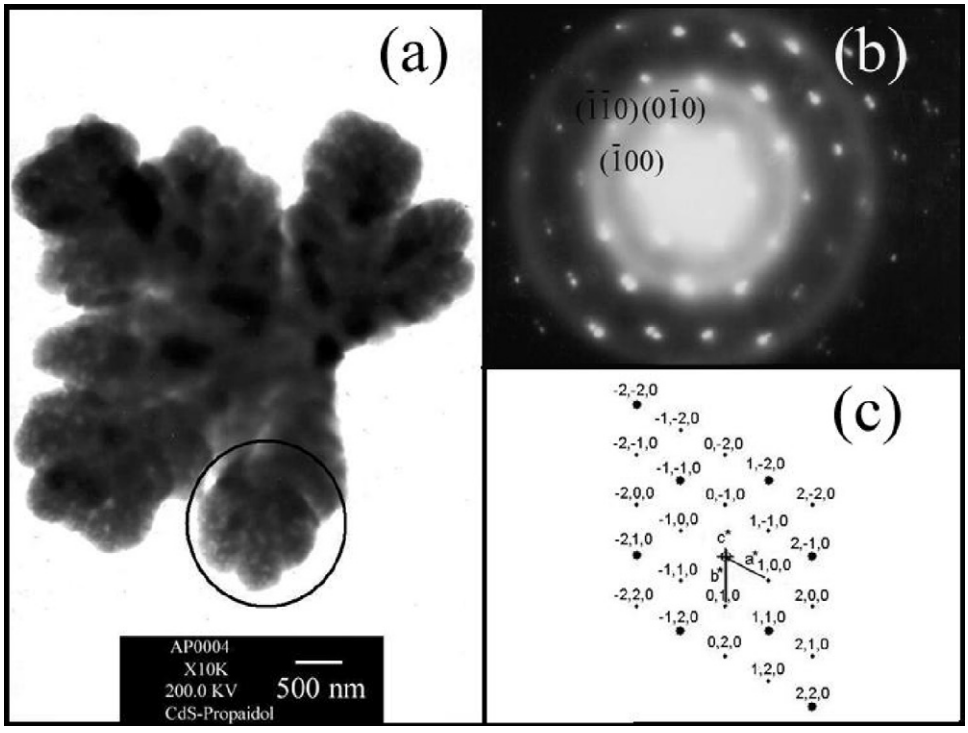

Fig. 4. (a) TEM image, and (b and c) SAED and simulated patterns of CdS synthesized at 200 °C for 10 h.

diameter. Sometimes, the clusters were broken, caused by their internal stress.

To synthesize CdS round microparticles in flower-like clusters in the autoclaves at 100–200 °C, $CdCl_2$ and thiourea (NH_2CSNH_2) possibly formed Cd–thiourea complex in propylene glycol. The complex was thermally decomposed and hexagonal CdS was synthesized [21]. The hexagonal unit cells of CdS clustered together to form a number of nanoparticles, composing round microparticles. Growths in all directions were almost at the same rates to synthesize round microparticles. Their sizes were limited to 1 μm diameter by the pressure inside the autoclaves. Formation and clustering of microparticles simultaneously proceeded to form flowers. Nucleation and growth of the particles can play roles in the product morphology. Crystal growth of some preferred structure or plane related to surface energy of the plane in the specified condition. The plane with lower surface energy was dominant. It was described as the shape selective surface absorption process [22]. Amount of the starting agents in the solution also had the influence on particle orientation which reflected nucleation and growth of crystals. Particle orientation was increased with the increase in the amount of starting agents [23]. Apart from the above, crystal growth was influenced by the precursor solubility in the particular solvent and test temperature, having the influence on the morphology [22]. High temperature played the role in the product morphology by enlarging the size of clusters. Polarities and boiling points of solvents [24], pH values of the solutions and others can play roles in the shapes and sizes due to the different rates of nucleation and growth. The fundamental microparticles may contain some defects, due to the growth rate, internal stress and others.

TEM image of CdS is shown in Fig. 4a. It was composed of a number of nanoparticles composing the microparticles in clusters. The TEM and SEM results were in good accordance. Its SAED pattern (Fig. 4b) characterized at a circle on the TEM image, appeared as systematic array of bright spots. They aligned as hexagons around the same center. These showed that a number of atoms aligned in their normal lattice sites. The interpreted pattern [11,25] specified as the $(\bar{1}00)$, $(\bar{1}\,\bar{1}\,0)$, and $(0\,\bar{1}\,0)$ planes, corresponding to CdS (hcp) [15]. Calculated electron beam [11,25] was in the [001] direction. It was the direction that electron beam was sent to the surface of the crystal. A diffraction pattern (Fig. 4c) for hexagonal CdS with a^*, b^* and c^* reciprocal lattice vectors in the [100], [010] and [001] directions, and electron beam in the [001] direction was also simulated [26]. The simulated spots were in symmetric and systematic order. Both simulated and interpreted patterns were in good accordance, although some spots of the interpreted pattern did not appear on the simulated one – as the following explanation. To simulate the pattern, intensity and size of the spots (planes) were mutually related. The stronger intensity was used, the larger size was achieved. The intensity and size of the spots were limited by a saturated intensity used for simulation. Thus the planes of the JCPDS database with low intensity did not appear in the simulated pattern. Diffusive concentric rings were also detected on the interpreted pattern. They were caused by the carbon grid on which the product was put for the analysis.

The quantitative of Cd and S elements was analyzed by EDX as shown in Fig. 5. The EDX spectrum revealed the presence of three peaks at 3.13, 3.32 and 3.53 keV, corresponding to the L_α, $L_{\beta1}$ and $L_{\beta2}$ lines of Cd atoms, respectively. The peak at 2.31 keV corresponded to $K_{\alpha1,2}$ line of S atoms. Cu from a Cu–C grid was also detected at 8.04 ($K_{\alpha1,2}$), 8.91 (K_β) and 0.93 (L_α) keV, and C at 0.28 ($K_{\alpha1,2}$) keV [27]. According to the EDX analysis, atomic ratio of Cd:S was 49:51, very close to the composition of CdS (hcp).

The absorption of hexagonal CdS round microparticles in flower-like clusters is shown in Fig. 6. The UV–visible spectra exhibited the absorption at 493–498 nm (2.49–2.51 eV) – blue shift relative to the bulk (515 nm), due to the quantum confinement effect [8,28,29].

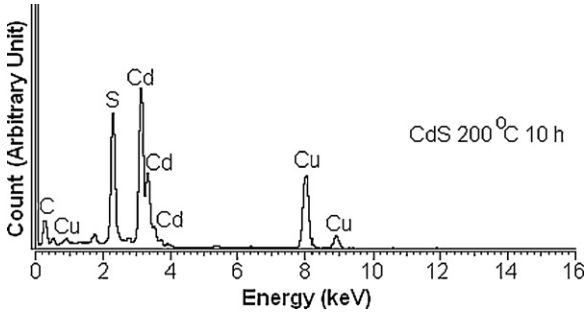

Fig. 5. EDX spectrum of CdS synthesized at 200 °C for 10 h.

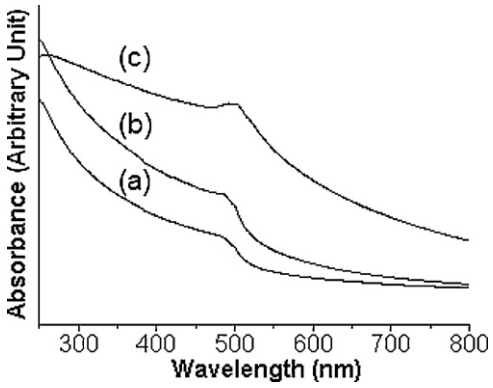

Fig. 6. UV–visible spectra of CdS synthesized at (a) 100 °C for 10 h, (b) 100 °C for 30 h, and (c) 200 °C for 10 h.

Photoluminescence (PL) property was involved in crystal structure of the materials, doping elements, and impurities in most cases or crystal defects. They were excited and taken part in the photonic emission. In case of CdS nanomaterial, negative-charge cadmium vacancies (V_{Cd}) and negative-charge sulphur interstitials (I_S) acted as acceptors, while positive-charge sulphur vacancies (V_S) and positive-charge cadmium interstitials (I_{Cd}) acted as donors. The PL emission has different transitions, namely (a) CB to VB transition, (b) free excitonic recombination, (c) excitons bound to neutral donors, (d) excitons bound to neutral acceptors, (e) donor–acceptor pairs, (f) green emission due to transition to I_S, (g) yellow emission due to I_{Cd}, (h) red emission due to V_S, and (i) transition from V_{Cd} to VB. Absorption of photons generated electrons and holes. These electrons were trapped in different interstitial sites and vacancies [30].

Photoluminescence (PL) of CdS synthesized under different conditions (Fig. 7) was at 431 nm wavelength near band edge, although their intensities were different, due to the recombination of

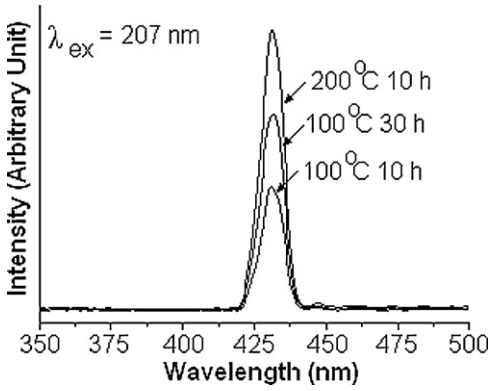

Fig. 7. PL spectra of CdS synthesized at different temperatures and lengths of time.

excitons and/or shallowly trapped electron–hole pairs [31]. It was blue shift as compared with the 512 nm of CdS (bulk) [32], due to the quantum confinement effect [31]. PL intensities were sensitive to the particle sizes. They were increased with the increase in the glycolthermal temperatures and lengths of time. For the product synthesized at 200 °C for 10 h, its PL intensity was the highest. The intensity was also very sensitive to the number of electronic transfers and defects in the products [33], which were influenced by the particle morphologies.

4. Conclusions

Wurtzite hexagonal CdS round microparticles in flower-like clusters were successfully synthesized by the 100–200 °C glycolthermal reactions in propylene glycol. Both X-ray and electron diffraction results were in good accordance to the same JCPDS database number. The corresponding constituents composing the phase exhibited the fundamental and overtone Raman modes at 296 and 595 cm^{-1}, respectively. PL emissions of the products were at the same wavelength of 431 nm, although their intensities were increased with the increase in the test temperatures and lengths of time.

Acknowledgements

We wish to thank the National Nanotechnology Center (NANOTEC), National Science and Technology Development Agency (NSTDA), Thailand, for providing financial support through the project code: P-10-11345 for Research, Development and Engineering (RD&E), and the Thailand's Office of the Higher Education Commission for providing financial support through the National Research University (NRU) Project, including Prince of Songkla University for the research funding.

References

[1] M. Chen, L. Pan, Z. Huang, J. Cao, Y. Zheng, H. Zhang, Mater. Chem. Phys. 101 (2007) 317–321.
[2] G. Tai, W. Guo, Ultrason. Sonochem. 15 (2008) 350–356.
[3] J.R. Lakowicz, I. Gryczynski, Z. Gryczynski, C.J. Murphy, J. Phys. Chem. B 103 (1999) 7613–7620.
[4] A. Datta, A. Saha, A.K. Sinha, S.N. Bhattacharyya, S. Chatterjee, J. Photochem. Photobiol. B 78 (2005) 69–75.
[5] T. Thongtem, A. Phuruangrat, S. Thongtem, J. Phys. Chem. Solids 69 (2008) 1346–1349.
[6] L. Wang, L. Chen, T. Luo, Y. Qian, Mater. Lett. 60 (2006) 3627–3630.
[7] Q. Pan, K. Huang, S. Ni, Q. Wang, F. Yang, D. He, Mater. Lett. 61 (2007) 4773–4776.
[8] W. Qingqing, Z. Gaoling, H. Gaorong, Mater. Lett. 59 (2005) 2625–2629.
[9] N.M. Huang, C.S. Kan, P.S. Khiew, S. Radiman, J. Mater. Sci. 39 (2004) 2411–2415.
[10] G. Li, L. Jiang, H. Peng, B. Zhang, Mater. Lett. 62 (2008) 1881–1883.
[11] T. Thongtem, A. Phuruangrat, S. Thongtem, Mater. Lett. 61 (2007) 3235–3238.
[12] D. Andreescu, E. Matijević, D.V. Goia, Colloids Surf. A 291 (2006) 93–100.
[13] C. Feldmann, Solid State Sci. 7 (2005) 868–873.
[14] D.R. Lide (Editor-in-Chief), CRC Handbook Chem. Phys., CRC Press, Boca Raton, FL, 2005, pp. 3–484, 5–35, 6–3. http://www.hbcpnetbase.com.
[15] Powder Diffract. File, JCPDS-ICDD, 12 Campus Boulevard, Newtown Square, PA 19073-3273, U.S.A., 2001.
[16] K. Aup-Ngoen, S. Thongtem, T. Thongtem, Mater. Lett. 65 (2011) 442–445.
[17] Y. Keereeta, T. Thongtem, S. Thongtem, J. Alloys Compd. 509 (2011) 6689–6695.
[18] C. Suryanarayana, M.G. Norton, X-ray Diffract. A Pract. Appro., Plenum Press, New York, 1998.
[19] H.M. Fan, X.F. Fan, Z.H. Ni, Z.X. Shen, Y.P. Feng, B.S. Zou, J. Phys. Chem. C 112 (2008) 1865–1870.
[20] C. Li, X. Yang, B. Yang, Y. Yan, Y. Qian, J. Cryst. Growth 291 (2006) 45–51.
[21] D. Chen, K. Tang, G. Shen, J. Sheng, Z. Fang, X. Liu, H. Zheng, Y. Qian, Mater. Chem. Phys. 82 (2003) 206–209.
[22] S. Biswas, S. Kar, S. Chaudhuri, J. Cryst. Growth 299 (2007) 94–102.
[23] Y.C. Zhang, X.Y. Hu, T. Qiao, Solid State Commun. 132 (2004) 779–782.
[24] J. Lu, Q. Han, X. Yang, L. Lu, X. Wang, Mater. Lett. 61 (2007) 2883–2886.
[25] K.W. Andrews, D.J. Dyson, S.R. Keown, Interpret. Electr. Diffract. Patterns, Plenum Press, New York, 1971.
[26] C. Boudias, D. Monceau, CaRIne Crystallography 3.1, DIVERGENT S.A., Centre de Transfert, 60200 Compiègne, France, 1989–1998.
[27] X-ray Absorp. Emiss. Energ., Oxford Instrum. Analyt., Halifax Rd., High Wycombe Bucks HP12 3SE, UK. www.oxford-instruments.com.
[28] Y.C. Zhang, G.Y. Wang, X.Y. Hu, J. Alloys Compd. 437 (2007) 47–52.
[29] P. Bera, C.H. Kim, S.I. Seok, Solid State Sci. 12 (2010) 532–535.
[30] V. Singh, P. Chauhan, J. Phys. Chem. Solids 70 (2009) 1074–1079.
[31] M. Salavati-Niasari, F. Davar, M.R. Loghman-Estarki, J. Alloys Compd. 481 (2009) 776–780.
[32] A.M. Qin, Y.P. Fang, W.X. Zhao, H.Q. Liu, C.Y. Su, J. Cryst. Growth 283 (2005) 230–241.
[33] M. Alonso, E.J. Finn, Fundamental University Phys., vol. 3, Addison-Wesley Publ. Co., MA, 1968.